Divergence of Function in the Hot Dog Fold Enzyme Superfamily: The Bacterial Thioesterase YciA[†]

Zhihao Zhuang,[‡] Feng Song,[‡] Hong Zhao,[‡] Ling Li,[‡] Jian Cao,[‡] Edward Eisenstein,[§] Osnat Herzberg,[§] and Debra Dunaway-Mariano*[,‡]

Department of Chemistry, University of New Mexico, Albuquerque, New Mexico 81713, and Center for Advanced Research in Biotechnology, University of Maryland Biotechnology Institute, Rockville, Maryland 20850

Received November 26, 2007; Revised Manuscript Received January 9, 2008

ABSTRACT: Thioesters play a central role in the cells where they participate in metabolism, membrane synthesis, signal transduction, and gene regulation. Thioesters are converted to the thiol and carboxylic acid components by thioesterase-catalyzed hydrolysis. Here we examine the biochemical and biological function of the hot dog fold thioesterase YciA (EcYciA) from *Escherichia coli* and its close sequence homologue HI0827 from *Haemophilus influenzae* (HiYciA). The quaternary structure of HiYciA was determined, using equilibrium sedimentation techniques, to be a homohexamer. Mass spectral and ^{31}P NMR analysis of purified HiYciA revealed a bound CoA ligand. Kinetic analyses showed that CoA is a strong feedback inhibitor. YciA thioesterase activity toward acyl-CoA substrates was determined using steady-state kinetic methods. The k_{cat} and k_{cat}/K_m values obtained reveal a striking combination of high catalytic efficiency and low substrate specificity. The substrate activity of propionyl-s-*N*-acetylcysteine was found to be negligible and that of *n*-butyryl-pantetheinephosphate low, and therefore, it is evident YciA does not target acylated ACPs or other acylated proteins as substrates. The results from bioinformatic analysis of the biological distribution and genome contexts of *yciAs* are reported. We conclude that YciA is responsible for the efficient, "seemingly" indiscriminant, CoA-regulated hydrolysis of cellular acyl-CoA thioesters in a wide range of bacteria and hypothesize that this activity may support membrane biogenesis.

Thioesters play a central role in the cells where they participate in metabolism, membrane synthesis, signal transduction, and gene regulation (*1*). The carboxylic acid components of biological thioesters are metabolites of varied size, shape, and polarity. They are converted to thioesters by ligases for the purpose of solubility, transport, signaling, or activation for reaction in biosynthetic or biodegradation pathways. The naturally occurring thiols include coenzyme A (CoA),[1] glutathione, the pantetheine unit of the holoacyl carrier protein (ACP), and the cysteine residue of a protein. Thioesters are reverted to the thiol and carboxylic acid components by hydrolysis catalyzed by thioesterases. Thioesterases have primarily evolved within the α/β-fold hydrolase enzyme superfamily (*2*) and the hot dog fold enzyme superfamily (*3*). The conserved fold of the hot dog fold superfamily proteins consists of a five-stranded antiparallel β-sheet wrapped around an elongated α-helix. This topology is reminiscent of a hot dog "bun" wrapping around a "sausage", hence the name hot dog fold (*4*).

Following the discovery of the first hot dog fold thioesterase (viz., the 4-hydroxybenzoyl-CoA thioesterase from *Pseudomonas* sp. strain CBS3) (*5*), we embarked on a long-term study of the diversification of function within the hot dog fold thioesterase family (*6–14*). During the course of this work, we have discovered that (i) the hot dog fold is conserved despite the low degree of amino acid sequence conservation within the family,[2] (ii) divergent evolution within this family is based on two rather than one catalytic scaffold (*6*), (iii) there is no conservation of a set of core catalytic residues and, instead, one carboxylate residue [Asp or Glu located at either of two positions of the catalytic scaffold (*6, 12*)] operates within a variety of sequence contexts, and (iv) the absence of well-defined, desolvated substrate binding pockets is responsible for low substrate specificity (*13*). These family features combine in such a way to severely impede a sequence-based, and even a three-dimensional structure-based, approach to function assignment. It is for this reason that we have focused our attention on a set of hot dog thioesterases that are produced by the well-characterized organism *Escherichia coli* so that we may use gene context, as well as the knowledge of metabolic pathways and known

[†] This work was supported by National Institutes of Health Grants P01 GM57890 (O.H.) and R01 GM28688 (D.D.-M.).

* To whom correspondence should be addressed: Department of Chemistry and Chemical Biology, University of New Mexico, Albuquerque, NM 81713. Telephone: (505) 277-3383. Fax: (505) 277-6202. E-mail: dd39@unm.edu.

[‡] University of New Mexico.

[§] University of Maryland Biotechnology Institute.

[1] Abbreviations: DTNB, 5,5′-dithiobis(2-nitrobenzoic acid); CoA, coenzyme A; DTT, dithiothreitol; IPTG, isopropyl β-D-thiogalactopyranoside; PMSF, phenylmethanesulfonyl fluoride; K$^+$Hepes, potassium salt of *N*-(2-hydroxyethyl)piperazine-*N*′-2-ethanesulfonate; ACP, acyl carrier protein; 4-HBA-CoA, 4-hydroxybenzoyl-coenzyme A; SDS−PAGE, sodium dodecyl sulfate−polyacrylamide gel electrophoresis.

[2] For example, the pairwise sequence alignment of *E. coli* YciA with YbgC (14% identical), YbaW (8% identical), YbdB (17% identical), YdiI (15% identical), and PaaI (13% identical) reveals no significant sequence homology.

10.1021/bi702334h CCC: $40.75 © 2008 American Chemical Society
Published on Web 02/02/2008

protein components of cellular processes, to guide the discovery of thioesterase biochemical and biological function.

There are seven different hot dog thioesterases encoded by the *E. coli* genome, and each has a known X-ray structure. However, only one of these thioesterases has been assigned a biological function. It is PaaI (PDB entry 2fs2; Swiss-Prot entry P76084), which we discovered to participate in the phenylacetate degradation pathway to free CoA from the product of the first pathway reaction, phenylacetyl-CoA, in the event that downstream pathway enzymes are not present (*12*). The other six hot dog thioesterases are YciA (b1253; Swiss-prot entry P0A8Y8) (PDB entry 1yli of the *Haemophilus influenzae* homologue HI0827; Swiss-prot entry P44886) YbgC (b0534; PDB entry 1s5u; Swiss-prot entry P0A8Z3), YbaW (b0443; PDB entry 1njk; Swiss-prot entry P77712), YbdB (b0579; PDB entry 1vh9; Swiss-prot entry P0A8Y8), YdiI (b1686; PDB entry 1vi8; Swiss-prot entry P77781), and the double-domain hot dog thioesterase TEII (b0452; PDB entry 1c8u; Swiss-prot entry P0AGG2).

Here, we report data that define the substrate range and CoA-directed regulation of YciA activity in *E. coli* and *H. influenzae*. Also, we present the results from a bioinformatics study of the phylogenetic distribution of YciA and the variation in *yciA* genetic context. We conclude that YciA is responsible for the efficient, "seemingly" indiscriminant hydrolysis of cellular acyl-CoA thioesters in a wide range of bacteria and hypothesize that this activity may support membrane biogenesis. In the following paper (*15*), we describe the three-dimensional structures of wild-type and mutant *H. influenzae* YciA (HI0827), and identify the structural basis for substrate binding, catalytic turnover, and CoA-directed regulation.

MATERIALS AND METHODS

Materials. All oligonucleotide primers and restriction enzymes, and the T4 DNA ligase, were purchased from Gibco BRL. DNA sequencing was performed by the DNA Sequencing Facility of the University of New Mexico. All biochemicals, including a majority of the acyl-CoAs, were purchased from Sigma. The propionyl-s-*N*-acetylcysteamine was prepared as previously described (*7*), as were 4-hydroxybenzoyl-CoA, 4-hydroxyphenylacetyl-CoA, and 3-hydroxyphenylacetyl-CoA (*12*). The protocols for the synthesis of hexyl-CoA and *n*-butyryl-pantetheinephosphate are reported in the Supporting Information. The protein concentration was determined by using the Bradford method.

Gene Cloning. The genes encoding YciA in *H. influenzae* (HI0827; Swiss-Prot entry P44886) and YciA in *E. coli* (Swiss-Prot entry P0A8Z0) were amplified by PCR using *PfuTurbo*DNA polymerase (Stratagene) and the clone GHI or the clone 10798D-5 obtained from ATCC (Manassas, VA). Primers containing restriction endonuclease cleavage sites *Nde*I and *Xho*I were used. The amplification protocol employed 30 cycles of denaturation at 95 °C, annealing at 45 °C, and elongation at 72 °C. The pET-23b vector (Novagen), which was cut with the restriction enzymes 5′-*Nde*I and 3′-*Xho*I, was ligated to the isolated gene. The ligation product was used to transform *E. coli* JM109 competent cells (Stratagene). Plasmid was prepared using a QIAprep Spin Miniprep Kit (Qiagen). The gene sequence was confirmed by DNA sequencing. The recombinant plasmid was used to transform *E. coli* BL21(DE3) competent cells (Novagen). The transformed cells were grown at 32 °C in 1.5 L of Luria-Bertani broth containing 50 μg/mL carbenicillin to an an OD_{600} of ~0.8 and then induced using 0.4 mM IPTG until an OD_{600} of ~2.0 was reached.

Purification of Recombinant YciA. (1) HiYciA. The cells (*vide infra*) were harvested by centrifugation, and the cell pellet was suspended in ice-cold 50 mM K^+Hepes (pH 7.5) containing 2 mM DTT and 0.2 mM PMSF. The cells were lysed in a French press cell at 1200 psi, and the lysate was centrifuged. The supernatant was loaded onto a (5 cm × 40 cm) DEAE Sepharose Fast Flow column (Amersham Pharmacia Biotech) equilibrated with 50 mM K^+Hepes buffer (pH 7.5). A 0 to 0.5 M linear gradient of KCl in 50 mM K^+Hepes (pH 7.5) was used to elute the protein. The desired fractions (eluted at 0.1 M KCl) were pooled and concentrated. The concentrated protein solution was subjected to ammonium sulfate fractionation. The 40−60% (w/v) ammonium sulfate fraction was centrifuged, and the protein pellet was dissolved in 2 mL of 10 mM K^+Hepes buffer (pH 7.5) containing 0.15 M KCl. The protein solution was loaded onto a (2 cm × 100 cm) Sephacryl-S 200 column and eluted with 10 mM K^+Hepes (pH 7.5) containing 0.15 M KCl. The desired fractions were combined and concentrated. The protein remained fully active after prolonged storage at −80 °C. The homogeneous HiYciA protein [see the SDS−PAGE gel (Figure 1 of the Supporting Information)] is obtained in a yield of 50 mg of protein/g of wet cells.

(2) EcYciA. The cells (*vide infra*) were harvested by centrifugation and then suspended in 100 mL of ice-cold lysis buffer [50 mM NaH_2PO_4, 300 mM NaCl (pH 8.0), 10 mM imidazole, and 1 mM DTT] containing 10 μL of 0.1 mM PMSF, passed through a French press at 1200 psi, and then centrifuged at 48000*g* and 4 °C for 30 min. The supernatant was loaded onto a Ni-NTA agarose column (QIAGEN, 25 mL) pre-equilibrated with the lysis buffer. The column was first washed with 500 mL of a 50 mM NaH_2PO_4/300 mM NaCl/50 mM imidazole/1 mM DTT mixture (pH 8.0), and then the YciA was eluted with 200 mL of a 50 mM NaH_2PO_4/300 mM NaCl/250 mM imidazole/1 mM DTT mixture (pH 8.0). The fractions were analyzed by SDS−PAGE and then selectively pooled and concentrated using a Centricon (10 kDa, Pall Filtron) at 4 °C. The concentrate was chromatographed on a 2 cm × 180 cm Sephacryl-S 100 size exclusive column using a 50 mM NaH_2PO_4/50 mM NaCl/10 mM imidazole/1 mM DTT mixture (pH 8.0, 4 °C) as the eluant. The desired fractions were combined and concentrated. The homogeneous EcYciA protein [see the SDS−PAGE gel (Figure 1 of the Supporting Information)] is obtained in a yield of 25 mg of protein/g of wet cells.

^{31}P NMR Analysis of HiYciA. The proton-decoupled ^{31}P NMR spectra were recorded with a Bruker AC-F 500 NMR spectrometer at 202.5 MHz and 5 °C. The instrument was calibrated with 85% phosphoric acid.

Electrospray Ionization Mass Spectroscopy of HiYciA. Mass spectral determinations were carried out by the University of New Mexico Mass Spectroscopy Center. The protein was diluted in 10% acetonitrile, 90% water, and 0.1% formic acid and loaded into a NewObjective PicoTip. The solution was infused into an ion trap mass spectrometer (Finnigan LCQ DUO). The distance between the spray needle

and counter electrode was 3 mm. A voltage of 7.0 kV was applied at the spray needle.

Determination of the Steady-State Kinetic Constants for YciA-Catalyzed Acyl-CoA Thioester Hydrolysis. Reactions were monitored at 25 °C by measuring the 412 nm absorbance of 5-thio-2-nitrobenzoate formed by reaction of DTNB with the CoA, pantetheinephosphate, or *N*-acetylcysteine liberated from the acyl-CoA, acyl-pantetheinephosphate, or acyl(*N*-acetyl)cysteine substrate, respectively. Reactions were initiated by adding YciA to assay solutions composed of substrate, DTNB (1 mM), KCl (0.2 M), and 50 mM K^+Hepes (pH 7.5) and contained in quartz cuvettes (1 cm light path). Reaction solutions prepared with long chain acyl-CoA substrates (=C_8) also included bovine serum albumin in a 1:2 molar ratio with substrate.

The kinetic parameters V_{max} and K_m were determined from initial velocity data, measured as a function of substrate concentration, by using eq 1 and KinetAsyst (IntelliKinetics).

$$V = V_{max}[A]/([A] + K_m) \quad (1)$$

where [A] is the substrate concentration, V is the initial velocity, V_{max} is the maximum velocity, and K_m is the Michaelis constant. The reported error was computed for the data fitting. The k_{cat} was calculated from the ratio of V_{max} and the total enzyme concentration. The enzyme concentration was determined by using the Bradford method.

Determination of the Time Course for YciA-Catalyzed 4-HBA-CoA Hydrolysis. (1) Direct Assay. HiYciA (40 μM) was reacted with 4-HBA-CoA (50 μM) in the 50 mM K^+Hepes/0.15 M KCl buffer (pH 7.5, 25 °C). The reaction was monitored by measuring the decrease in solution absorbance at 300 nm, which is due to the disappearance of substrate 4-HBA-CoA ($\epsilon = 11.8$ mM^{-1} cm^{-1}).

(2) Continuous Assay. HiYciA (1.5 μM) was reacted with 4-HBA-CoA (50 μM) in the 50 mM K^+Hepes/0.15 M KCl/1 mM DTNB buffer (pH 7.5, 25 °C). The reaction progress was monitored by measuring the increase in the solution absorbance at 412 nm ($\epsilon = 13.6$ mM^{-1} cm^{-1}), which is due to the formation of the DTNB-derived 5-thio-2-nitrobenzoate.

Determination of Inhibition Constants. The inhibition constants were determined for YciA inhibitors at pH 7.5 and 25 °C by measuring the initial velocity of YciA-catalyzed acyl-CoA thioester hydrolysis as a function of substrate ($0.5-5 \times K_m$) and inhibitor ($1-3 \times K_{is}$) concentration. The initial velocity data were analyzed using eq 2 for competitive inhibition or eq 3 for mixed-type inhibition and the computer program KinetAsyst (IntelliKinetics).

$$V = V_{max}[S]/[K_m(1 + [I]/K_i) + [S]] \quad (2)$$

$$V = V_{max}[S]/[K_m(1 + [I]/K_{is}) + [S](1 + [I]/K_{ii})] \quad (3)$$

where V is the initial velocity, V_{max} is the maximum velocity, [S] is the substrate concentration, K_m is the Michaelis constant, [I] is the inhibitor concentration, and K_{is} and K_{ii} are the slope and intercept inhibition constants, respectively.

Determination of E. coli Growth Curves. E. coli K-12 strain (BW25113) and the corresponding *yciA*-knockout strain (JW1245) were obtained from the *E. coli* Genetic Stock Center of Yale University (New Haven, CT). JW1245 cells were grown aerobically at 37 °C in 2 L of LB medium containing 15 μg/mL kanamycin. BW25113 cells were cultured under the same conditions but without the kanamycin. The optical density of the cell culture was monitored at 600 nm.

RESULTS AND DISCUSSION

Physical Properties of EcYciA and HiYciA. Homogeneous recombinant HiYciA and His_6-tagged EcYciA were prepared as described in Materials and Methods (the SDS−PAGE gels are shown in Figure 1 of the Supporting Information). The predicted molecular mass of the His_6-tagged EcYciA is 15166 Da. The mass determined by electrospray ionization mass spectroscopy is 15163 Da. The predicted molecular mass of HiYciA is 16763 Da. The mass determined by electrospray ionization mass spectroscopy is 16632 Da, which indicates that the N-terminal Met is removed (−131 Da) by posttranslational modification. The quaternary structure of HiYciA was determined, using equilibrium sedimentation techniques (Figure 2 of the Supporting Information), to be a homohexamer.

The 154-amino acid HiYciA and 132-amino acid EcYciA are 69% identical in sequence. On the basis of the sequence alignment, HiYciA contains an additional five-amino acid segment near the N-terminus and an additional 17-amino acid segment at the C-terminus. The HiYciA is a highly soluble, robust protein, whereas the EcYciA tends to precipitate at high concentrations. Thus, most characterizations of YciA were carried out using HiYciA. The EcYciA was characterized to the extent that a comparison could be made between the enzymes to show generality in kinetic behavior.

The UV absorbance spectra of EcYciA and HiYciA reflected the maximum absorbance at 268 nm, which is reminiscent of nucleic acid absorbance; however, the treatment of the HiYciA with polyethyleneimine to induce precipitation of nucleic acids did not alter the absorbance maximum (see Figure 3 of the Supporting Information). The UV absorbance of the filtrate generated by centrifugal size filtration revealed a small molecule with an absorbance maximum of 260 nm. The LC−MS analysis of HiYciA carried out under denaturing conditions identified the protein at 16632 Da and a low-molecular mass species at 768 Da. The molecular mass of CoA is 767.5 Da. To verify the structure of the ligand, the proton-decoupled ^{31}P NMR spectrum of HiYciA was measured (see Figure 1). The spectrum of the protein sample contains a broad singlet at +5.85 ppm and a broad doublet at −9.40 ppm. The ^{31}P NMR spectrum of solvated CoA contains a sharp singlet at +5.05 ppm (3′-phosphate) and a doublet of doublets centered at −9.36 ppm (5′-pyrophosphate). The 0.8 ppm downfield shift and peak broadening observed for the signals from the HiYciA sample are consistent with the assignment of enzyme-bound CoA (*9*). Together, these findings show that YciA is copurified with a tightly bound CoA ligand.

Substrate Specificity of EcYciA and HiYciA. YciA thioesterase activity toward acyl-CoA substrates was determined using steady-state kinetic methods. The k_{cat} and k_{cat}/K_m values reported in Table 1 (HiYciA) and Table 2 (EcYciA) reveal a striking combination of high catalytic efficiency and low substrate specificity. Almost all of the k_{cat}/K_m values measured are within what might be considered to be a "physiologically relevant" range (viz., $k_{cat}/K_m > 10^4$ M^{-1} s^{-1}). HiYciA is somewhat more active than EcYciA, displaying

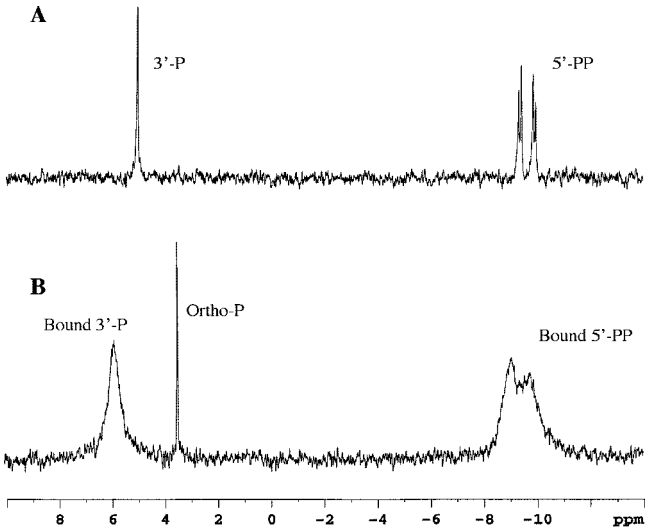

FIGURE 1: (A) ^{31}P NMR spectrum of 1 mM CoA at pH 7.5 and 25 °C. (B) ^{31}P NMR spectrum of purified HiYciA (1 mM) at pH 7.5 and 25 °C. Orthophosphate was used as the internal standard (+3.46 ppm).

for its best substrates k_{cat}/K_m values between 1×10^7 and 1×10^8 M^{-1} s^{-1}, and k_{cat} values between 100 and 200 s^{-1}. The long, medium, and short chain fatty acyl-CoAs are very good substrates as are the small acyl-CoA metabolites that were tested. The slowest substrate is 4-hydroxybenzoyl-CoA. Apparently, the juxtaposition of the aromatic ring and the C(=O) reaction center impairs binding and/or catalysis. The competitive inhibition constant (K_i) of the inert 4-hydroxybenzoyl-CoA analogue 4-hydroxyphenacyl-CoA [the C(=O)SCoA group is replaced with $C(=O)CH_2SCoA$] was determined for HiYciA to be 5.8 ± 0.3 μM (Figure 4 of the Supporting Information). This suggests that the 4-hydroxybenzoyl-CoA binds tightly to YciA but is not optimally aligned for the hydrolysis reaction. Indeed, the k_{cat} measured for 4-hydroxybenzoyl-CoA hydrolysis is 3 orders of magnitude smaller than that measured for 4-hydroxyphenylacetyl-CoA hydrolysis (in this substrate, a methylene group separates the aromatic ring from the thioester C=O group).

The substrate activities of propionyl-s-*N*-acetylcysteine (Table 1) and *n*-butyryl-pantetheinephosphate (Table 2) were tested to determine if YciA requires CoA as the substrate thiol unit. Propionyl-CoA is efficiently hydrolyzed with a k_{cat}/K_m of 4.2×10^6 M^{-1} s^{-1}, whereas propionyl-s-*N*-acetylcysteine is not hydrolyzed at a detectable rate. Thus, the *N*-acetylcysteine unit is not compatible with the substrate-binding site. The *n*-butyryl-pantetheinephosphate is a slow substrate for HiYciA and EcYciA (Tables 1 and 2). In the case of EcYciA, a direct comparison can be made between the activity of *n*-butyryl-CoA and *n*-butyryl-pantetheinephosphate (Table 2) to show that the k_{cat}/K_m is reduced 1000-fold and the k_{cat} is reduced 82-fold by removal of the 3′,5′-adenosine bisphosphate moiety from the *n*-butyryl-CoA substrate. We conclude that YciA recognizes acyl-CoAs but not acylated ACPs or other acylated proteins as substrates.

To access the importance of the thioester C=O group in substrate binding, we measured the competitive inhibition constant of the hexanoyl-CoA (for HiYciA, $k_{cat} = 15$ s^{-1} and $K_m = 4$ μM) analogue hexyl-CoA (thioester C=O group replaced with a CH_2 group). The tight binding that was observed [for HiYciA, $K_i = 1.9 \pm 0.2$ μM; for EcYciA, $K_i = 5.4 \pm 0.5$ μM (Figure 5 of the Supporting Information)] suggests that the substrate thioester C=O group does not contribute significantly to the substrate binding energy.

Product Inhibition by EcYciA and HiYciA. The high catalytic efficiency of YciA toward most cellular acyl-CoA metabolites presents a potential danger to the cell. We therefore looked for known cell export sequence motifs within the YciA gene but found none. Likewise, no evidence that YciA is localized at the cell membrane by a transmembrane helix or a palmitoyl appendage was found. Assuming that YciA is a cytoplasmic enzyme, it follows that there must exist some form of cellular regulation to prevent YciA from hydrolyzing all of the acyl-CoA metabolites present in the cytoplasm. CoA product inhibition was suggested by the observation that YciA is purified from the cell with CoA bound (*vide infra*). The effectiveness at which CoA serves as a feedback inhibitor was evaluated in two ways. First, we showed that the kinetic behavior of the purified enzyme, which contains bound CoA, is distinctly different from that of YciA, which had been freed from its CoA ligands. The time course for the HiYciA-catalyzed hydrolysis of propionyl-CoA, measured using the continuous DTNB-based spectrophotometric assay for CoA formation (Figure 2A), reveals an initial lag in product formation when the reaction is initiated by adding the enzyme to the assay solution containing substrate and DTNB. In contrast, there is no such lag observed for the time course of the reaction initiated by adding substrate to the assay solution containing enzyme and DTNB. This result shows that for HiYciA to be fully active the bound CoA must be removed, which was accomplished by preincubation of the enzyme with DTNB. Second, we showed that the time course for the catalyzed hydrolysis of 4-hydroxybenzoyl-CoA measured in the presence of DTNB (measured using a 40-fold lower enzyme concentration) reflects a rate and product yield higher than those measured in the absence of DTNB (Figure 2B). The same experiment, carried out with EcYicA, produced similar results (data not shown).

Because CoA inhibition could not be assessed directly, we used the CoA analogue desulfoCoA (CH_2SH is replaced by CH_3) to obtain an estimate of the CoA inhibition constant. Noncompetitive inhibition of HiYciA-catalyzed isobutyryl-CoA hydrolysis was observed (Figure 6 of the Supporting Information) which defined a K_{ii} of 4.7 ± 0.8 μM (V_{max} altered) and a K_{is} of 0.33 ± 0.04 μM (V_{max}/K_m altered). This result suggests that the CoASH analogue competes with isobutyryl-CoA for the substrate binding site (the V_{max}/K_m effect) and that it also combines to a form of the enzyme that does not bind isobutyryl-CoA (the V_{max} effect). Specifically, desulfoCoA may bind the binary YciA(isobutyrate) product complex to generate the "dead-end" YciA(isobutyrate)(desulfoCoA) complex. Alternatively, desulfoCoA may mimic CoA as a potential allosteric regulator, a topic that is examined in the following paper (*15*).

The desulfoCoA K_{is} of 0.33 μM is evidence that CoA binds very tightly to YciA, more tightly than do the S-alkylated CoA substrate analogues (*vide infra*). The crystal structure of the CoA-bound HiYciA described in the following paper (*15*) shows that the CoA thiol group fits exceptionally well within a hydrophobic niche adjacent to the active site cleft. Because the desulfoCoA lacks the thiol group, its K_{is} value might be an underestimate of the actual CoA binding affinity.

Table 1: Steady-State Kinetic Constants for *H. influenzae* YciA (HI0827)-Catalyzed Hydrolysis of Acyl-CoA Thioesters at pH 7.5 and 25 °C Determined Using the DTNB Spectrophotometric Assay (see Materials and Methods for details)

substrate	k_{cat} (s^{-1})	K_m (μM)	k_{cat}/K_m (M^{-1} s^{-1})
acetyl-CoA	1.3 ± 0.1	4.7 ± 0.9	2.7×10^5
propionyl-CoA	25 ± 10	6 ± 1	4.2×10^6
propionyl-s-*N*-acetylcysteamine	<0.0001	−	−
n-butyryl-CoA	22 ± 1	3.5 ± 0.2	6.2×10^6
n-hexanoyl-CoA	15 ± 1	4.1 ± 0.5	3.6×10^6
n-octanoyl-CoA	4.6 ± 0.2	1.9 ± 0.3	2.4×10^6
n-decanoyl-CoA	13 ± 1	4.5 ± 0.5	2.8×10^6
lauroyl-CoA	9.2 ± 0.3	6.6 ± 0.7	1.4×10^6
myristoyl-CoA	6.9 ± 0.1	2.5 ± 0.1	2.8×10^6
palmitoyl-CoA	2.7 ± 0.1	17 ± 1	1.6×10^5
stearoyl-CoA	0.77 ± 0.02	10 ± 1	7.5×10^4
arachidoyl-CoA	0.27 ± 0.01	39 ± 1	6.9×10^3
palmitoleoyl-CoA	5.7 ± 0.2	6.4 ± 0.8	8.9×10^5
oleoyl-CoA	1.7 ± 0.1	11 ± 1	1.5×10^5
linoleoyl-CoA	2.0 ± 0.1	4.2 ± 0.1	4.7×10^5
D,L-β-hydroxybutyryl-CoA	8.3 ± 0.2	31 ± 2	2.7×10^5
isobutyryl-CoA	140 ± 10	13 ± 1	1.1×10^7
n-butyryl-pantethienephosphate	0.8 ± 0.02	1400 ± 100	5.7×10^2
isovaleryl-CoA	30 ± 1	14 ± 2	2.1×10^6
tiglyl-CoA	2.6 ± 0.1	2.1 ± 0.2	1.3×10^6
β-methylcrotonyl-CoA	0.54 ± 0.03	9 ± 1	6.0×10^4
crotonyl-CoA	0.92 ± 0.03	5.9 ± 0.4	1.5×10^5
methylmalonyl-CoA	1.1 ± 0.1	170 ± 0.1	6.3×10^3
malonyl-CoA	3.3 ± 0.2	140 ± 20	2.4×10^4
succinyl-CoA	190 ± 10	20 ± 3	9.5×10^6
glutaryl-CoA	100 ± 10	8.1 ± 0.6	1.3×10^7
D,L-3-hydroxy-3-methylglutaryl-CoA	8.9 ± 0.4	20 ± 2	4.5×10^5
acetoacetyl-CoA	35 ± 1	37 ± 2	9.4×10^5
4-HBA-CoA	0.078 ± 0.003	9.1 ± 0.9	8.6×10^3
phenylacetyl-CoA	130 ± 10	1.6 ± 0.1	8.3×10^7
4-hydroxyphenylacetyl-CoA	75 ± 3	7.6 ± 0.8	9.9×10^6
3-hydroxyphenylacetyl-CoA	140 ± 0.10	3.7 ± 0.5	3.7×10^7

Table 2: Steady-State Kinetic Constants for *E. coli* YciA-Catalyzed Hydrolysis of Acyl-CoA Thioesters at pH 7.5 and 25 °C Determined Using the DTNB Spectrophotometric Assay (see Materials and Methods for details)

substrate	k_{cat} (s^{-1})	K_m (μM)	k_{cat}/K_m (M^{-1} s^{-1})
acetyl-CoA	0.55 ± 0.01	167 ± 4	3.3×10^3
n-butyryl-CoA	6.7 ± 0.4	68 ± 1	9.9×10^4
n-butyryl-pantethienephosphate	0.082 ± 0.003	800 ± 80	1.0×10^2
isobutyryl-CoA	9.5 ± 0.7	15 ± 2	6.3×10^5
n-decanoyl-CoA	17 ± 2	13 ± 3	1.3×10^6
lauroyl-CoA	9.6 ± 0.6	20 ± 3	4.9×10^5
oleoyl-CoA	13.0 ± 0.5	11 ± 1	1.2×10^6
palmitoyl-CoA	3.7 ± 0.1	33 ± 1	1.1×10^5
β-methylcrotonyl-CoA	0.10 ± 0.01	290 ± 50	3.7×10^2
4-HBA-CoA	0.0062 ± 0.0002	25 ± 2	2.4×10^3
phenylacetyl-CoA	9.4 ± 0.7	16 ± 3	6.0×10^5

Exceptionally tight CoA binding has not been reported for other hot dog thioesterases. The CoA inhibition constants measured for the 4-hydroxybenzoyl-CoA thioesterases (of the 4-chlorobenzoate degradation pathway) from *Arthrobacter* sp. strain SU and *Pseudomonas* sp. strain CBS3 are as follows: $K_{is} = 29\,\mu M$ and $K_{is} = 370\,\mu M$, respectively (*9, 10*).

To determine if the carboxylate product formed in the HiYciA-catalyzed hydrolysis of the acyl-CoA substrate contributes to YciA regulation via product inhibition, the K_i values for a variety of alkanoates were measured (at pH 7.5 and 25 °C; DTNB-coupled assay) by using these compounds as competitive inhibitors of 4-hydroxybenzoyl-CoA hydrolysis. Among the nine compounds tested, decanoate shows the strongest inhibition with a K_{is} of 120 ± 15 μM. However, in view of the *n*-decanoyl-CoA K_m of 4.5 μM, we conclude that decanoate does not qualify as an effective feedback inhibitor. 4-Hydroxybenzoate ($K_{is} \sim 2$ mM), hexanoate ($K_{is} \sim 5$ mM), and octanoate ($K_{is} \sim 5$ mM) proved to be weak competitive inhibitors, whereas the K_{is} values of the short chain alkanoates acetate, proprionate, *n*-butyrate, D-(−)-β-hydroxybutyrate, and acetoxyacetate exceed 40 mM. These values contrast with the comparatively small K_m values measured for HiYciA-catalyzed hydrolysis of the corresponding acyl-CoA thioesters (Table 1).

YciA Phylogenic Distribution and Gene Context Analysis. The sequences of EcYciA and HiYciA (69% identical

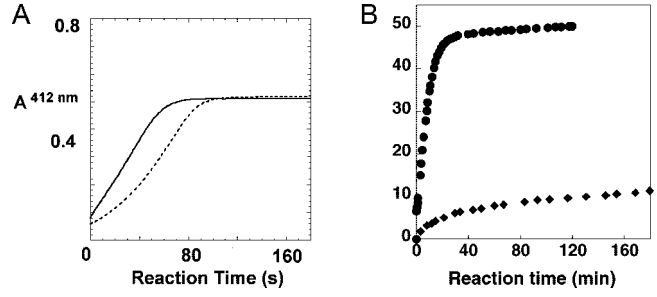

FIGURE 2: (A) Plot of reaction solution absorbance at 412 nm vs reaction time (seconds) that defines the time course for HiYciA (6 nM)-catalyzed hydrolysis of propionyl-CoA (30 μM) in a 50 mM K^+Hepes/0.15 M KCl buffer (pH 7.5, 25 °C) containing 1.5 mM DTNB: (---) reaction initiated by adding HiYciA to the assay solution and (—) reaction initiated by adding propionyl-CoA to the assay solution 2 min following the addition of HiYciA. (B) Plot of the concentration of coenzyme A (micromolar) formed in the reaction mixture vs reaction time (minutes). (●) The reaction mixture initially contained 1.5 μM HiYciA, 50 μM 4-HBA-CoA, and 1 mM DTNB in 50 mM K^+Hepes/0.15 M KCl buffer (pH 7.5, 25 °C). (◆) The reaction mixture initially contained 40 μM HiYciA and 50 μM 4-HBA-CoA in 50 mM K^+Hepes/0.15 M KCl buffer (pH 7.5, 25 °C).

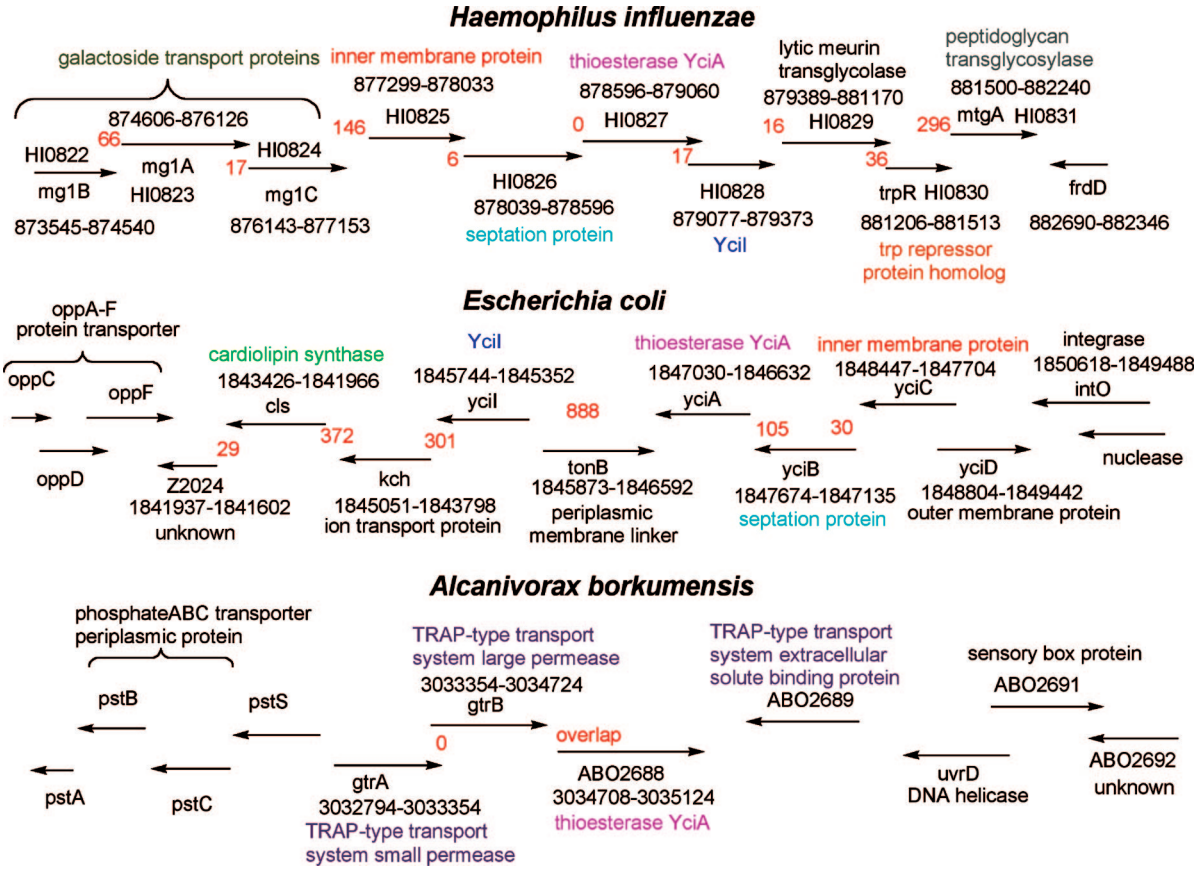

FIGURE 3: HiYciA and EcYciA gene contexts are depicted along with that of the YciA from *Alcanivorax borkumensis*. The DNA strand is indicated by the direction of the arrow; the gene size and genome location are given the nucleotide number above or below the arrow along with the gene name and annotation. The base number separation between adjacent genes is colored red.

sequence) were used as queries in BLAST (*16*) searches of the protein sequence nonredundant databank to define the biological range of YciA. The sequence homologues that are at least 60% identical with either of the query sequences are assumed to be orthologs. Homologues that fall in the 50–59% identity range are likely to be YciA orthologs, whereas we are less certain of homologues with a level of sequence identity in the range of 40–49% (see the sequence alignment in Figure 19 of the Supporting Information). In the Supporting Information, we detail the biological distribution of the YciA homologues that are >30% identical in sequence. Here we summarize these findings. YciA homologues are found in a wide distribution of bacteria and proteobacteria. However (with one exception, *Planctomyces maris*), the YciA homologues that fall within our definition of "certain ortholog" are found in bacteria that form the gamma division of proteobacteria and (with one exception, *Candidatus Blohmannia floridanus*) are present in all represented genera of Pasteurellaceae and Enterobacteriacea. We conclude that the biochemical function provided by YciA is a "general" one and not restricted to a "select group" of bacteria.

To explore how the YciA biochemical function might support the cell, the *yciA* gene context was examined using the annotated genomes of the bacterial species that contain a YciA homologue that is at least 50% identical insequence with EcYciA or HiYciA. The YciA gene neighborhoods of numerous proteobacteria are provided in the Supporting Information. Three representative maps are shown in Figure 3. For analysis, the guiding considerations include (i) two genes located on the same DNA strand that are separated by a short stretch of sequence (and are therefore likely to be cotranscribed and, thus, function in a common task) and (ii) two genes that have the same register on different DNA strands [and therefore might also perform a common task which is exemplified by the genes that encode the proteins required for the enterobactin synthesis, export, import, and cleavage that constitutes the machine for iron uptake in *E. coli* (*17*)].

As shown in Figure 3, the *H. influenzae yciA* gene is located on an operon. Although the function of this operon has not been determined, some of the genes that occur on and around this operon encode proteins that exhibit strong sequence homology to proteins of known biochemical and/or biological functions. These protein homologues provide clues about the cellular process that this operon supports. Specifically, several upstream gene neighbors (not shown in Figure 3) encode enzymes which form peptidoglycan precursors (for example, UTP-glucose-1-phosphate uridylyltransferase, galactokinase, and galactose-1-phosphate uridylyltransferase). These genes are followed by an operon that encodes the ABC transporter complex mglABC involved in galactose import. Located within the YciA operon is a gene that encodes a soluble periplasmic murein transglycolase (HI0829), which functions in the recycling of peptidoglycan muropeptides during cell elongation and/or cell division via catalyzed cleavage of the β-1,4-glycosidic bond between *N*-acetylmuramic acid and *N*-acetylglucosamine residues. The gene encoding the peptidoglycan synthesizing enzyme monofunctional peptidoglycan transglycosylase (HI0831) directly follows the *yciA*-containing operon.

In addition to YciA (which we have shown to be a broad spectrum acyl-CoA thioeserase) and the periplasmic murein transglycolase, the *H. influenzae yciA*-containing operon encodes a transcriptional repressor HI0830 (a Trp operon repressor homologue), two inner membrane proteins (HI0825 and HI0826), and one cytoplasmic protein (HI0828), all of unknown function. HI0825 is a multipass inner membrane protein that is conserved in *H. influenza*, *Haemophilus somonus*, and *Pasteurella multocida* (see the Supporting Information). The *P. multocida* ortholog (PM0330), which is 35% identical in sequence with HI0825, is a member of the Pfam family, UPF0259, which also contains the *E. coli* YciC [*E. coli yciC* and *yciA* are gene neighbors (Figure 3)]. This 46-member Pfam family spans γ-proteobacteria and contains various *Salmonella*, *Shigella*, *Yreshina*, and *Pseudomonas* species. HI0825 and the Pfam UPF0259 members are multipass inner membrane proteins. By virtue of its gene context and the connection to the Pfam family, we assume that HI0825 and YciC perform the same function.

HI0826 is the counterpart to the *Shigella flexneri* virulence factor ispA (YciB in *E. coli*), which is termed the cell "septation protein". The ispA is a small, integral inner membrane protein that when disrupted in *S. flexneri* causes gradual failure of cell division in the host epithelial cytoplasm, resulting in long filamentous forms which are unable to spread within the host cells (*18*). The process of septal invagination is arrested in the *in vivo* filamentous forms, whereas the *in vitro* cells display a normal phenotype. The role that ispA plays in cell division within the host cell is not known (*18*).

YciI is a small cytoplasmic protein that has a structure suggestive of an enzyme; however, we have not yet been successful in identifying its physiological substrate (*19*). The *yciI* gene is frequently coupled with *yciB* with or without the inclusion of *yciA*. YciI is observed as a fusion protein with BolA in *Coxiella burnetii*. BolA is required for normal cell morphology under conditions of stress, and it has been suggested that it is a regulator of cell wall biosynthesis and that it is a disulfide reductase (*20–22*).

In *E. coli*, the genes *yciA*, *yciB*, *yciC*, and *yciI* are juxtaposed, but unlike in the yciA-containing operon of *H. influenzae*, they are not located adjacent to the peptidoglycan remodeling genes (see Figure 3). Instead, the gene that encodes cardiolipin synthase is in the neighborhood. Cardiolipin synthase functions to increase the level of cardiolipin in the cell membrane, which in turn results in increased membrane fluidity. Membrane fluidity affects the function of integral membrane proteins (*23*). Cardiolipin also functions to organize the membrane protein partners, such as the proteins of a membrane transporter, into a functional complex (*24*) and to recruit proteins to the poles and septa of the inner membrane (*25*). Notably, among these recruited proteins are the cell cycle and septation peripheral proteins DnaA and MinD.

The *E. coli* cluster of *yciA*, *yciB*, *yciC*, and *yciI* genes is in register with genes on the opposing DNA strand which encode the oppA-F protein transporter, the periplasmic membrane linker protein tonB, and the outer membrane protein yciD. Together, this cluster encodes a protein export system that is used for protein excretion. An analogous gene arrangement is observed in other closely related genera such as *Samonella*, *Photorabus*, *Erwina*, *Shigella*, and *Buchnera* (see the Supporting Information).

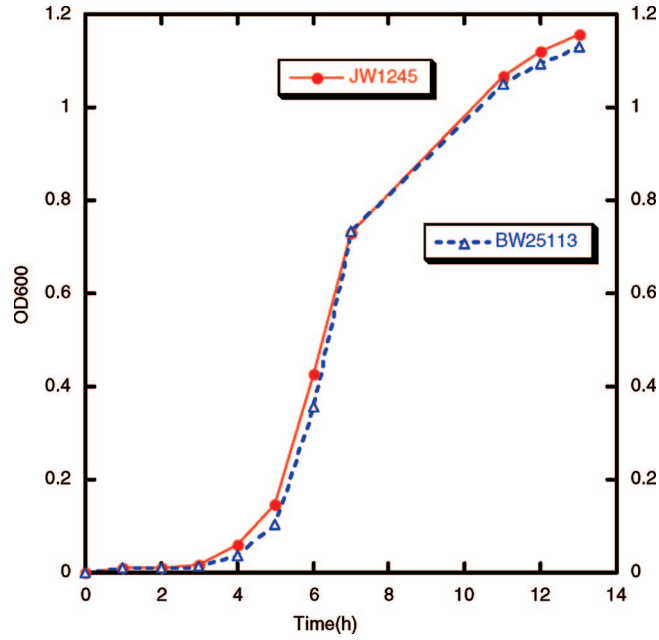

FIGURE 4: Plot of the culture optical density at 600 nm vs the cultivation time (hours) measured for the aerobic growth of the wild-type *E. coli* K-12 strain (BW25113) (blue) and *E. coli* yciA-knockout strain JW1245 (red) in LB medium at 37 °C.

A third gene cluster of particular interest is found in the genome of the more distantly related organism, *Alcanivorax borrkumensis* (Figure 3). Here *yciA* is located in an operon that encodes the synthesis of the TRAP-type transport system (tripartite ATP-independent periplasmic system). The TRAP is an active transporter, which functions in conjunction with an extracytoplasmic solute-binding receptor to import small organic metabolites (*27*).

In summary, YciA occurs in a variety of gene contexts, only a few of which we have described here, yet the emerging common theme is suggestive of the involvement of YciA in the biogenesis of the inner membrane for division or insertion of transport proteins.

YciA and E. coli Cell Survival under Optimal Aerobic Growth Conditions. To determine whether YciA is required for *E. coli* survival, we measured the growth curves for wild-type *E. coli* K-12 and for the corresponding *yciA*-knockout mutant strain. The growth curves (Figure 4) are identical. Thus, under optimal growth conditions, the absence of YciA does not appear to impede the rate of cell multiplication. This result is consistent with a previous study (*18*), which showed that a *S. flexneri* mutant strain lacking a functional septation protein gene displayed the abnormal growth phenotype (filament formation) only under *in vivo* conditions (i.e., inside cultured mammalian host cells) or under oxidative stress-inducing (*in vivo*-like) *in vitro* conditions.

Divergence of Function among E. coli Hot Dog Thioesterases. The *E. coli* cell produces seven hot dog thioesterases. In what way(s) does YciA distinguish itself from the other six thioesterases? Considering the gene context, *ybdB* is a member of the enterobactin-based iron acquisition gene locus, *ydiI* is a member of the cysteine sulfur recruitment/iron−sulfur cage synthesis gene cluster (viz., the suf operon), *ybgC* is a member of the Pal-tol septation ring gene locus, *ybaW* is a member of a peptide generation/export gene locus, *tesB* (encodes TE-II)

is not located in a recognizable function gene locus, and *paaI* is a member of the phenylacetate degradation operon.

The substrate ranges of the *E. coli* hot dog fold thioesterases also differ. YbgC and YbdB have low hydrolytic activity with acyl-CoAs (*7, 29*), and protein–protein binding partner analyses (*28, 29*) suggest that the physiological substrates are acylated-pantetheine-modified proteins. PaaI hydrolyzes phenylacetyl-CoA and its mono- and dihydroxy ring analogues, but not aliphatic acyl-CoAs (*12*). The substrate ranges of YbaW and YdiI have not, to our knowledge, been reported. The substrate range of TE-II is, like that of YciA, reported to be broad with regard to acyl-CoA thioester metabolites but, unlike that of YciA, includes acylated ACPs (*30*).

It is clear that each of the seven *E. coli* hot dog fold thioesterases performs a unique biological function. Our goal is to determine the biological functions of these thioesterases and to identify the elements in their structures that support these functions. In the following paper (*15*), we examine the structure of HiYciA.

SUPPORTING INFORMATION AVAILABLE

Text describing synthesis of *n*-butyryl-pantetheinephosphate, synthesis of *n*-hexyl-CoA, treatment of purified HI0827 protein sample with polyethyleneimine, HiYciA sedimentation equilibrium studies, and YciA phylogenetic distribution analysis and figures containing SDS−PAGE gel data, HiYciA sedimentation equilibrium data, steady-state inhibition data, and gene neighborhood maps. This material is available free of charge via the Internet at http://pubs.acs.org.

REFERENCES

1. Hunt, M. C., and Alexson, S. E. (2002) The role Acyl-CoA thioesterases play in mediating intracellular lipid metabolism. *Prog. Lipid Res. 41*, 99–130.
2. Nardini, M., and Dijkstra, B. W. (1999) Alpha/beta hydrolase fold enzymes: The family keeps growing. *Curr. Opin. Struct. Biol. 9*, 732–737.
3. Dillon, S. C., and Bateman, A. (2004) The Hotdog fold: Wrapping up a superfamily of thioesterases and dehydratases. *BMC Bioinf. 5*, 109–124.
4. Leesong, M., Henderson, B. S., Gillig, J. R., Schwab, J. M., and Smith, J. L. (1996) Structure of a dehydratase-isomerase from the bacterial pathway for biosynthesis of unsaturated fatty acids: Two catalytic activities in one active site. *Structure 4*, 253–264.
5. Benning, M. M., Wesenberg, G., Liu, R., Taylor, K. L., Dunaway-Mariano, D., and Holden, H. M. (1998) The three-dimensional structure of 4-hydroxybenzoyl-CoA thioesterase from *Pseudomonas* sp. strain CBS-3. *J. Biol. Chem. 273*, 33572–33579.
6. Thoden, J. B., Zhuang, Z., Dunaway-Mariano, D., and Holden, H. M. (2003) The structure of 4-hydroxybenzoyl-CoA thioesterase from *Arthrobacter* sp. strain SU. *J. Biol. Chem. 278*, 43709–43716.
7. Zhuang, Z., Song, F., Martin, B. M., and Dunaway-Mariano, D. (2002) The YbgC protein encoded by the ybgC gene of the tol-pal gene cluster of *Haemophilus influenzae* catalyzes acyl-coenzyme A thioester hydrolysis. *FEBS Lett. 516*, 161–163.
8. Thoden, J. B., Holden, H. M., Zhuang, Z., and Dunaway-Mariano, D. (2002) X-ray crystallographic analyses of inhibitor and substrate complexes of wild-type and mutant 4-hydroxybenzoyl-CoA thioesterase. *J. Biol. Chem. 277*, 27468–27476.
9. Zhuang, Z., Song, F., Zhang, W., Taylor, K., Archambault, A., Dunaway-Mariano, D., Dong, J., and Carey, P. R. (2002) Kinetic, Raman, NMR, and site-directed mutagenesis studies of the *Pseudomonas* sp. strain CBS3 4-hydroxybenzoyl-CoA thioesterase active site. *Biochemistry 41*, 11152–11160.
10. Zhuang, Z., Gartemann, K. H., Eichenlaub, R., and Dunaway-Mariano, D. (2003) Characterization of the 4-hydroxybenzoyl-coenzyme A thioesterase from *Arthrobacter* sp. strain. *Appl. Environ. Microbiol. 69*, 2707–2711.
11. Zhuang, Z., Song, F., Takami, H., and Dunaway-Mariano, D. (2004) The BH1999 Protein of *Bacillus halodurans* C-125 Is Gentisyl-Coenzyme A Thioesterase. *J. Bacteriol. 186*, 393–399.
12. Song, F., Zhuang, Z., Finci, L., Dunaway-Mariano, D., Kniewel, R., Buglino, J. A., Solorzano, V., Wu, J., and Lima, C. D. (2006) Structure, function, and mechanism of the phenylacetate pathway hot dog-fold thioesterase PaaI. *J. Biol. Chem. 281*, 11028–11038.
13. Cheng, Z., Song, F., Shan, X., Wei, Z., Wang, Y., Dunaway-Mariano, D., and Gong, W. (2006) Crystal structure of human thioesterase superfamily member 2. *Biochem. Biophys. Res. Commun. 349*, 172–177.
14. Song, F., Zhuang, Z., and Dunaway-Mariano, D. (2007) Structure-activity analysis of base and enzyme-catalyzed 4-hydroxybenzoyl coenzyme A hydrolysis. *Bioorg. Chem. 35*, 1–10.
15. Willis, M. A., Zhuang, Z., Song, F., Howard, A., Dunaway-Mariano, D., and Herzberg, O. (2007) Structure of YciA from *Haemophilus influenzae* (HI0827), a hexameric broad specificity acyl-CoA thioesterase. *Biochemistry 47*, 2797–2805.
16. Altschul, S. F., Madden, T. L., Schäffer, A. A., Zhang, J., Zhang, Z., Miller, W., and Lipman, D. J. (1997) Gapped BLAST and PSI-BLAST: A new generation of protein database search programs. *Nucleic Acids Res. 25*, 3389–3402.
17. Raymond, K. N., Dertz, E. A., and Kim, S. (2003) Enterobactin: An archetype for microbial iron transport. *Proc. Natl. Acad. Sci. U.S.A. 100*, 3584–3588.
18. Mac Siomoin, R. A., Nalata, N., Murai, T., Yoshikawa, M., Tsuji, H., and Sasakawa, C. (1996) Identification and characterization of ispA, a *Shigella flexneri* chromosomal gene essential for normal in vivo cell division and intercellular spreading. *Mol. Microbiol. 19*, 599–609.
19. Willis, M. A., Song, F., Zhuang, Z., Krajewski, W., Chalamasetty, V. R., Reddy, P., Howards, A., Dunaway-Mariano, D., and Herzberg, O. (2005) Structure of YciI from *Haemophilus influenza* (HIO828) reveals a ferredoxin-like α/β-fold with a histidine/aspartate centered catalytic site. *Proteins 59*, 648–652.
20. Santos, J. M., Freire, P., Vincente, M., and Arraiano, C. M. (1999) The stationary-phase morphogene *bolA* from *Escherichia coli* is induced by stress during early stages of growth. *Mol. Microbiol. 32*, 789–798.
21. Santos, J. M., Lobo, M., Matos, A. P., De Pedro, M. A., and Arraiano, C. M. (2002) The gene bolA regulates *dacA* (PBP5), *dacC* (PBP6) and *ampC* (AmpC), promoting normal morphology in *Escherichia coli*. *Mol. Microbiol. 45*, 1729–1740.
22. Huynen, M. A., Spronk, C. A. E. M., Gabaldon, T., and Snel, B. (2005) Combining data from genomes, Y2H and 3D structures indicates that BolA is a reductase interacting with a glutaredoxin. *FEBS Lett. 579*, 591–596.
23. Bernal, P., Segura, A., and Ramos, J.-L. (2007) Compensatory role of the cis-trans-isomerase and cardiolipin synthase in the membrane fluidity of *Pseudomonas putida* DOT-T1E. *Environ. Microbiol. 9*, 1658–1664.
24. Mileykovskaya, E. (2007) Subcellular localization of *Escherichia coli* osmosensory transporter ProP: Focus on cardiolipin membrane domains. *Mol. Microbiol. 64*, 1419–1422.
25. Romantsov, T., Helbig, S., Culham, D. E., Gill, C., Stalker, L., and Wood, J. M. (2007) Cardiolipin promotes polar localization of osmosensory transporter ProP in *Escherichia coli*. *Mol. Microbiol. 64*, 1455–1465.
26. Bernal, P., Munoz-Rojas, J., Hurtado, A., Ramos, J. L., and Segura, A. (2007) A *Pseudomonas putida* cardiolipin synthesis mutant exhibits increased sensitivity to drugs related to transport functionality. *Environ. Microbiol. 9*, 1135–1145.
27. Rabus, R., Jack, D. L., and Kelly, D. J., Jr. (1999) TRAP transporters: An ancient family of extra cytoplasmic solute-receptor-dependent secondary active transporters. *Microbiology 145*, 3431–3445.
28. Leduc, D., Battesti, A., and Bouveret, E. (2007) The hotdog thioesterase EntH (YbdB) plays a role in vivo in optimal enterobactin biosynthesis by interacting with the ArCP domain of EntB. *J. Bacteriol. 189*, 7112–7126.
29. Gully, D., and Bouveret, E. A. (2006) Protein network for phospholipid synthesis uncovered by a variant of the tandem affinity purification method in *Escherichia coli*. *Proteomics 6*, 282–293.
30. Naggert, J., Narasimhan, M. L., DeVeaux, L., Cho, H., Randhawa, Z. I., Cronan, J. E., Jr., Green, B. N., and Smith, S. (1991) Cloning, sequencing, and characterization of *Escherichia coli* thioesterase II. *J. Biol. Chem. 266*, 11044–11050.

BI702334H